JACS
JOURNAL OF THE AMERICAN CHEMICAL SOCIETY
Article
pubs.acs.org/JACS

Scaling of Polymer Dynamics at an Oil–Water Interface in Regimes Dominated by Viscous Drag and Desorption-Mediated Flights

Dapeng Wang,[†] Renfeng Hu,[‡] Joshua N. Mabry,[†] Bing Miao,[§] David T. Wu,[‡] Kaloian Koynov,[∥] and Daniel K. Schwartz*[,†]

[†]Department of Chemical and Biological Engineering, University of Colorado, Boulder, Colorado 80309, United States
[‡]Department of Chemistry and Geochemistry, Colorado School of Mines, Golden, Colorado 80401, United States
[§]College of Materials Science and Optoelectronic Technology, University of Chinese Academy of Sciences, Beijing 100049, China
[∥]Max Planck Institute for Polymer Research, Ackermannweg 10, 55128 Mainz, Germany

Supporting Information

ABSTRACT: Polymers are found near surfaces and interfaces in a wide range of chemical and biological systems, and the structure and dynamics of adsorbed polymer chains have been the subject of intense interest for decades. While polymer structure is often inferred from dynamic measurements in bulk solution, this approach has proven difficult to implement at interfaces, and the understanding of interfacial polymer conformation remains elusive. Here we used single-molecule tracking to study the interfacial diffusion of isolated poly(ethylene glycol) molecules at oil–water interfaces. Compared to diffusion in dilute aqueous solution, which exhibited the expected dependence of the diffusion coefficient (D) upon molecular weight (M) of $D \sim M^{-1/2}$ for a Gaussian chain, the behavior at the interface was approximately $D \sim M^{-2/3}$, suggesting a significantly more expanded polymer conformation, despite the fact that the oil was a poor solvent for the polymer. Interestingly, this scaling remained virtually unchanged over a wide range of oil viscosity, despite the fact that at low viscosities the magnitude of the diffusion coefficient was consistent with expectations based on viscous drag (i.e., Stokes–Einstein diffusion), and for high viscosity oil, the interfacial mobility was much faster than expected and consistent with the type of intermittent hopping transport observed at the solid–liquid interface. The dependence on molecular weight, in both regimes, was consistent with results from both self-consistent field theory and previous Monte Carlo simulations, suggesting that an adsorbed polymer chain adopted a partially swollen (loop–train–tail) interfacial conformation.

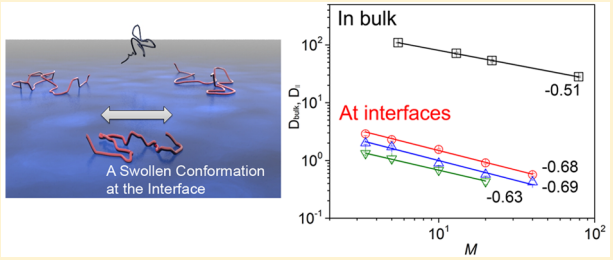

INTRODUCTION

The conformation of flexible polymer chains is a classic topic in polymer physics with broad technological implications, from plastic/rubber fabrication to protein folding and DNA transcription/replication.[1] Qualitatively, the conformation of individual polymer chains depends on the interactions with the surrounding solvent, where chains are expanded in a good solvent and condensed in a poor solvent. In the context of Flory's mean field theory,[2] this is often expressed using an approximate power law relation, of $R_g \propto M^{\nu}$, between the radius of gyration R_g and the molecular weight M. In this expression, the Flory exponent, ν, depends on the quality of the solvent. For example, under so-called θ-conditions, the conformation of individual polymer chains satisfies random walk statistics (ν = 0.5), while in "good" solvent, a polymer chain can be modeled approximately as a self-avoiding walk, leading to ν = 0.6 in three dimensions or ν = 0.75 in two dimensions.[1]

Although polymer conformations in dilute solutions have been thoroughly characterized,[1,3] the conformation and dynamics of polymers at interfaces are less well understood.[4] Some previous studies have focused on polymer motion at a solid–liquid surface, often attempting to relate the motion to molecular conformation. This approach is challenging for several reasons. For example, polymer surface conformations are presumably influenced by polymer–surface interactions, and since solid surfaces often exhibit rare but anomalously strong binding sites[5] due to surface heterogeneity,[4k,6] one may observe spatially heterogeneous mobility as well, complicating the interpretation of motion. Moreover, in contrast to the behavior in dilute solution, where polymer conformation (i.e., the hydrodynamic radius) can be derived from the diffusion coefficient D using the Stokes–Einstein relation, the connection between surface diffusion and conformation is less clear and potentially more complex. For example, independent laboratories have recently found that polymers exhibited intermittent hopping at the liquid–solid interface,[7] and a desorption-mediated mechanism has been proposed to describe this motion.[8] In this model, surface dynamics are closely related to the characteristic waiting time between desorption-mediated

Received: July 8, 2015
Published: September 8, 2015

DOI: 10.1021/jacs.5b07108
J. Am. Chem. Soc. 2015, 137, 12312–12320

flights. Thus, even after decades of intensive study, the understanding of interfacial polymer conformation remains elusive, in part due to the issues described above. Importantly, many of these difficulties can be reduced by employing a liquid−liquid interface, where polymer chains interact with a surface that is spatially homogeneous. Previous studies indicated that protein and small molecule diffusion was Brownian at the aqueous interface with low viscosity oil, but exhibited hopping diffusion at the interface with high viscosity oil.[9] In the Brownian regime, diffusion can be directly related to the liquid viscosities and an effective hydrodynamic radius; the connection between hopping diffusion and polymer conformation is less clear. However, by employing classic theories based on the relation between the desorption energy and the number of adsorbed monomers,[4m,10] hopping diffusion can be used as a complementary means to understand the interfacial polymer conformation.

Here, we aimed to address the question of polymer conformation at an oil−water interface using high-throughput molecular tracking. Specifically, we studied a series of poly(ethylene glycol) (PEG) chains with varying molecular weights at the interface between water and polydimethylsiloxane (PDMS) oil. Consistent with previous studies,[9] we observed a transition from Brownian to hopping diffusion by increasing the oil viscosity by more than 2 orders of magnitude. Here, we focused on the scaling of diffusion with molecular weight in these distinct diffusion regimes. In the Brownian regime, where diffusion was dominated by viscous drag, the Stokes−Einstein relation allowed us to convert a well-defined diffusion coefficient to an apparent hydrodynamic radius. In the hopping diffusion regime, however, a deviation from Stokes−Einstein behavior, along with a non-Gaussian step-size distribution and subdiffusive motion, suggested that interfacial diffusion was dominated by intermittent desorption-mediated flights requiring a different model to connect diffusion and molecular conformation. Interestingly, while the scaling with molecular weight of the three-dimensional (3D) diffusion in the aqueous phase was consistent with a Gaussian chain conformation (i.e., θ-solvent conditions), the behavior at the oil−water interface exhibited a distinctly different dependence on molecular weight (consistent with a more swollen conformation), regardless of the oil viscosity. SCFT[11] and the classical theory[4m,10] of adsorbed flexible chains were used to connect the interfacial conformation to diffusion, in both diffusive regimes, suggesting that the interface acted as an effective good solvent environment. This consistency, across two distinct diffusive regimes, provided a comprehensive picture of the conformation of adsorbed polymer chains in the context of interfacial transport.

EXPERIMENTAL METHODS

Materials. PDMS was obtained from Dow Corning, with viscosities of 92, 708, and 11042 cP, respectively. Water used for sample preparation and cleaning was Milli-Q water with resistivity of 18.2 MΩ·cm. Amine-terminated PEG for the single-molecular tracking measurements was purchased from Nanocs USA, with molecular weights of 3.4, 5, 10, 20, and 40 kg/mol, provided by the manufacturer. Alexa 488 NHS (Molecular Probes, Inc.) was used to react with amine-terminated PEG using a protocol suggested by the manufacturer. Alexa 488 was carefully selected over numerous other dyes to react with amine-terminated PEG because the adsorption rate of the isolated fluorophore was vanishingly low. The fluorescently labeled PEG with molecular weights of 3.4 and 5 kg/mol were purified from residual free fluorescent dyes using multiple repetitions of high-performance liquid chromatography. For PEG with molecular weights of 10, 20, and 40 kg/mol, the free dye was removed using multiple passes through desalting columns (Thermo Scientific). A control measurement showed that the desalting column and HPLC had equal separation quality.

Sample Preparation. To study PEG diffusion at the PDMS−water interface, glass coverslips were cleaned using UV-ozone treatment for 1 h, rinsed using Milli-Q water, and dried in a clean nitrogen stream. A drop of PDMS was placed on a coverslip and stabilized using a nickel TEM grid, as described previously.[12] Subsequently, approximately 800 μL of PEG solution was carefully added on top of the PDMS surface.

Single-Molecule Tracking. Single-molecule tracking measurements at PDMS-water interfaces were performed using an objective-based Nikon Ti-E total internal reflection fluorescence microscope (TIRFM) in conjunction with a 100× oil immersion objective. The refractive indices of the objective oil, glass slide, and PDMS were 1.52, 1.52, and 1.4, respectively. Therefore, in order to achieve total internal reflection at the oil−water interface, the incident angle was adjusted to be within the range 61°− 67°. The measurements were performed at 22 °C unless noted otherwise. A cooled EMCCD camera (iXon DU897) operating at −80 °C was employed to capture sequences of images with an acquisition time of 0.05 s. Alexa 488 labeled PEG was excited using a 488 nm laser from Agilent Technologies (model MLC 400B). The PEG solutions were prepared at a concentration of 10^{-7}−10^{-8} mg/mL with phosphate buffered saline buffers to keep the average interfacial coverage below 0.01 molecule/μm^2, signifying that the measurements were performed in the dilute range where no polymer−polymer interactions were expected. TIRFM excites the fluorophores within a water layer of 100 nm adjacent to the interface. However, given the high diffusion coefficient in the dilute aqueous solutions (Figure 4), the diffusion of PEG in bulk water was beyond the resolution limit of TIRFM (i.e., molecules in the bulk aqueous phase were completely blurred and contributed only to the fluorescent background). For each measurement, more than 30 movies, each with 50 s duration, were continuously captured at multiple locations. The measurements were repeated on multiple days. The positions of labeled polymer were identified in each image, and molecular trajectories were extracted from the image sequences using a custom-developed tracking algorithm as described previously.[13] All of the statistical analyses were based on trajectories with residence times longer than 0.8 s. Moreover, we calculated the time-averaged mean squared displacement (MSD) of each trajectory $\overline{r^2(\Delta t)} = \frac{1}{t-\Delta t}\int_0^{T-\Delta t}(r(t+\Delta t)-r(t))^2 dt$, where T is the total measurement time of a given trajectory and Δt is the lag time. The plots of $\overline{r^2(\Delta t)}$ vs Δt were fitted by a linear model, $\overline{r^2(\Delta t)} = 4D_{\parallel,n}\,\Delta t$ over the first six data points to yield the diffusion coefficient of each trajectory ($D_{\parallel,n}$). The trajectories with the lowest 10% of $D_{\parallel,n}$, were identified as anomalously slow (likely due to aggregates or contaminants) and eliminated from subsequent analysis. We note that the scaling of the average $D_{\parallel}$ vs molecular weight was unchanged within experimental uncertainty when including these anomalously slow trajectories. However, for more sensitive subsequent quantitative analysis (e.g., power law behavior of MSD), it was important to exclude trajectories that did not clearly correspond to actual single PEG molecules.

Several measures were used to statistically characterize the dynamics. The ensemble-averaged step-size distribution, $G(\Delta x, \Delta t)$, was calculated using the expression:

$$G(\Delta x, \Delta t) = \frac{1}{N}\sum_{i=1}^{N}\langle\delta[\Delta x + x_i(t) - x_i(t+\Delta t)]\rangle$$

which indicates the probability of a molecule moving a distance Δx along the x coordinate in the time interval Δt. N is the total number of trajectories, and the bracket $\langle\ldots\rangle$ denotes the trajectory average. Also, the ensemble average MSD was calculated according to $\langle r(\Delta t)^2\rangle = \langle[r(t+\Delta t) - r(t)]^2\rangle$, where $r(t)$ denotes the position in the x−y plane at time t, and the brackets represent the ensemble average.

DOI: 10.1021/jacs.5b07108
J. Am. Chem. Soc. 2015, 137, 12312−12320

RESULTS

PEG Diffusion at the PDMS−Water Interface. As described above, the diffusion of PEG at interfaces between water and PDMS with viscosities (η_{oil}) of 92, 708, and 11042 cP was characterized using TIRFM with an acquisition time of 0.05 s (Figure 1a). PEG adsorption at PDMS−water interface is driven by the hydrophobic interaction.[14] Representative trajectories at different interfaces are illustrated in Figure 1b−d and exhibit qualitatively different behavior. In particular, the molecular motion at the interface with low viscosity oil was apparently consistent with a regular 2D random walk, while at the interface with the highest viscosity oil (Figure 1d), it evolved to exhibit intermittent behavior, with periods of clustered small steps and occasional longer jumps.

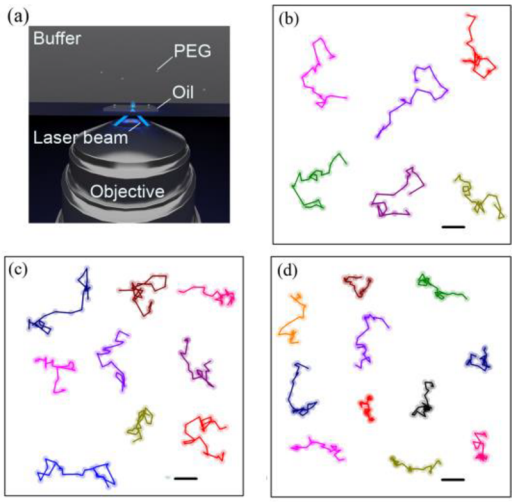

Figure 1. (a) Schematic representation of TIRFM at the oil−water interface. A laser beam (blue lines) is totally reflected at the interface between PDMS and water. An evanescent field is generated within which fluorophores are excited. Representative trajectories of 20 kg/mol PEG at the aqueous interface with PDMS with viscosity (b) 92, (c) 708, and (d) 11042 cP, respectively. The scale bar in (b−d) represents 1 μm.

A more detailed statistical analysis of the molecular trajectories confirmed that qualitatively different types of motion were observed at interfaces with oils of increasing viscosity. In particular, at the interface between water and the lowest viscosity PDMS (η_{oil} = 92 cP), the step-size distribution exhibited Gaussian statistics (Figure 2a), consistent with two-dimensional (2D) in-plane Brownian motion. However, with increasing oil viscosity, the step-size distribution systematically, and increasingly, deviated from Gaussian behavior. In particular, in comparing the measured step-size distributions to the Gaussian fits in Figure 2b,c, it was apparent that the experimental distributions were systematically broader and that the deviation became greater with increasing viscosity (Figure 2c). This was also seen in the residuals shown in Figure S3. This was particularly obvious for the highest viscosity oil and represented a quantitative signature of the intermittent motion described above. Similar behavior was observed for all molecular weights studied here, contrasting dramatically with the Gaussian distribution of step sizes expected for polymers undergoing simple 2D Brownian motion.[15] These analyses suggested the presence of two distinct mechanisms of interfacial diffusion: (1) 2D Brownian motion and (2) intermittent hopping and that Brownian motion was dominant at the interface with low viscosity oil while intermittent hopping dominated mobility when the oil was extremely viscous.

We also calculated the ensemble-average MSD versus Δt, as shown in Figure 3. Qualitatively, the systematic decrease of MSD with increasing molecular weight (along with the narrowing of the step-size distribution in Figure 2) consistently reflected the expected slowing of interfacial motion for larger polymer chains. For the interfaces with low and intermediate viscosity PDMS (η_{oil} = 92 and 708 cP), the MSD data could be adequately described by the relation $\langle r(\Delta t)^2 \rangle = 4D_{\|}\Delta t$, where $D_{\|}$ is the interfacial diffusion coefficient (solid lines in Figure 3a,b). If we attempted to fit these data to the more general expression $\langle r(\Delta t)^2 \rangle = 4D_{\|}\Delta t^n$, the data in Figure 3a yielded n = 1.00 ± 0.03, indicating that diffusion was Fickian at the interface with 92 cP PDMS, while n in the range of 0.94−1.00 was found for data in Figure 3b, indicating that polymer motion was very weakly subdiffusive at the interface with 708 cP PDMS. The MSD data for polymer diffusion at the interface with the highest viscosity PDMS (η_{oil} = 11042 cP) were weakly, but significantly, subdiffusive and required power law exponents in the range of 0.93−0.96 as annotated in Figure 3c.

Nevertheless, since the deviation from Gaussian behavior was relatively modest, to quantify $D_{\|}$ in a way that would permit self-consistent comparisons as a function of molecular weight and viscosity, we fit all MSD data to a linear model over the first 10 data points ($\Delta t \leq 0.5$s) where the linear relation was adequate. The dependence of $D_{\|}$ on M is shown in Figure 4a. Interestingly, even though the type of motion at different

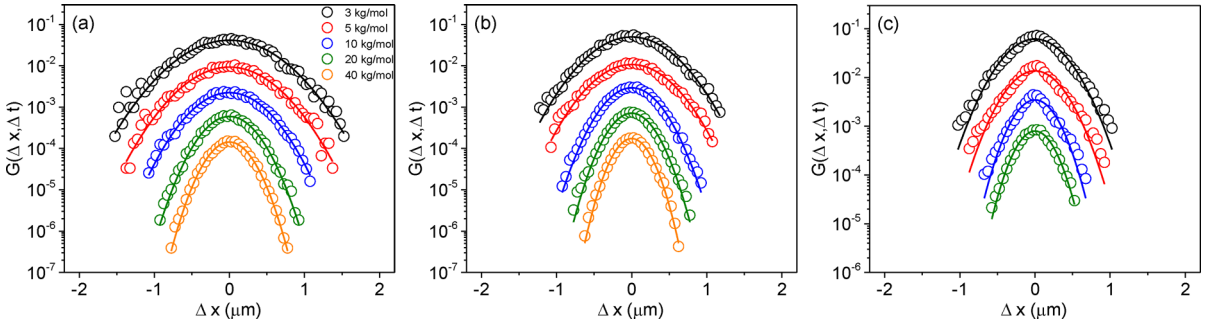

Figure 2. Step-size distributions for PEG with different molecular weights at the interface between an aqueous phase and PDMS with η_{oil} = (a) 92, (b) 708, and (c) 11042 cP for a time interval Δt = 0.05 s. The symbols denote experimental data. The solid lines represent Gaussian fits $G(\Delta x) = A \exp(-\Delta x^2/2\sigma^2)$, where A is the amplitude and σ^2 is the variance. To guide the eye, the data and curves were shifted downward by factors of 1/5, 1/25, 1/125, and 1/625 for PEG with molecular weights of 5, 10, 20, 40 kg/mol, respectively.

DOI: 10.1021/jacs.5b07108
J. Am. Chem. Soc. 2015, 137, 12312−12320

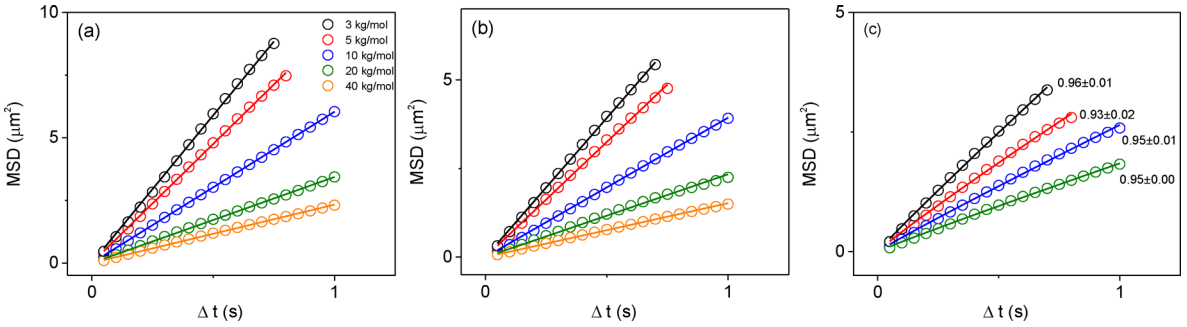

Figure 3. MDS vs lag time for PEG of various molecular weights at interface with PDMS viscosity η_{oil} = (a) 9, (b) 708, (c) 11402 cP, respectively. Symbols indicate experimental data. In (a) and (b), the solid lines represent linear fits by MSD = $4D\Delta t$. In (c), the solid lines represent power law fits, MSD = $4D\Delta t^n$; n for each plot is annotated at right.

interfaces was distinctly different, we found the scaling exponent of $D_{||}$ vs N yielded similar values that were all in the range of 0.63−0.69.

For the most viscous oil, data are not shown in Figure 4a for the highest molecular weight PEG. While the scaling exponent of $D_{||}$ vs M was unchanged within experimental uncertainty (−0.61 ± 0.03 compared to −0.63 ± 0.01) with the inclusion of these data, we found that the measurement of the apparent diffusion coefficient for this very slow-moving sample was unduly influenced by single-molecule localization error compared to the faster-moving systems, leading to unreliable comparisons overall.

Diffusion in Aqueous Solution. Fluorescence correlation spectroscopy (FCS)[16] was used to characterize the diffusion of Alexa 488 labeled PEG in aqueous solutions. The details of the measurements and typical autocorrelation curves (Figure S1) are shown in the Supporting Information. The diffusion of PEG in dilute aqueous solutions was well-described as Gaussian diffusion for the time intervals Δt studied and the diffusion coefficient, D_{bulk}, versus molecular weight, M, is shown in Figure 4a represented as open square symbols. The power law exponent was approximately −0.51, consistent with previous observations that isolated short PEG chains in aqueous solution are phenomenologically under θ-conditions and can be described by random walk statistics.[4e] Notably, this dependence on molecular weight was distinctly different from the behavior of the interfacial diffusion coefficient, $D_{||}$, which, as described above, exhibited a scaling exponent in the range 0.63−0.69 depending on oil viscosity.

Measured vs Theoretical Diffusion Coefficients. We compared the measured values of D_{bulk} and $D_{||}$ with the theoretical diffusion coefficient D_{SE} calculated by the relevant Stokes−Einstein equation:

$$D_{SE} = k_B T/6\pi\eta_{water}R_H \quad (1)$$

in aqueous solution, or

$$D_{SE} = 3k_B T/16R_H(\eta_{oil} + \eta_{water}) \quad (2)$$

at the oil−water interface (i.e., for a disk in two-dimensions)[17] where the apparent hydrodynamic radius, R_H, was extrapolated from the appropriate self-consistent field theory (SCFT calculations are detailed in Supporting Information). As shown in Figure 4b, $D_{bulk} = D_{SE}$ (open black squares in Figure 4b) and $D_{||} = D_{SE}$ for the interface with η_{oil} = 92 cP (open red circles in Figure 4b). However, at interfaces with more viscous PDMS oil (i.e., η_{oil} = 708 and 11042 cP), $D_{||}$ was significantly greater than the theoretically expected value, D_{SE}, that would be due to thermal motion and viscous drag. For the intermediate oil viscosity, the ratio $D_{||}/D_{SE}$ was approximately equal to 5, and this ratio increased to ∼50 for the interface with the most viscous PDMS (Figure 4b). These observations are qualitatively consistent with previous results for polymer, protein, and lipid diffusion at liquid interfaces,[9,18] where $D_{||}$ agreed with the Stokes−Einstein prediction for low oil viscosities but was anomalously large for high oil viscosities.

■ ANALYSIS AND DISCUSSION

The diffusion in bulk solution and at interfaces with low viscosity PDMS conformed to conventional "Stokes−Einstein" expectations, where diffusion is Fickian and the diffusion coefficient is a simple consequence of thermal motion and viscous drag. However, at interfaces with more highly viscous oil, polymer diffusion was anomalous in several ways and became increasingly anomalous with increasing oil viscosity. Based on the observations described above, we hypothesized that the dynamic polymer behavior at interfaces with highly viscous oil (11042 cP) was analogous to previously observed desorption-mediated dynamics of polymer chains at a solid−water interface.[4m] Clearly, it is intuitively reasonable that an oil−water interface should resemble a solid−water interface (with a hydrophobic solid) in the limit of highly viscous oil. Also, the polymers exhibited similar phenomenology (intermittent hopping and non-Gaussian step-size distributions) at solid−water interfaces and interfaces with the most viscous oil. Finally, the limiting value of the absolute diffusion coefficient at the interface with 11,042 cP PDMS was ∼0.4 $\mu m^2/s$, very similar to that observed at the solid−water interface.[4m,7a]

Taken together, the experimental evidence, including weak subdiffusion, anomalously fast interfacial diffusion, intermittent trajectories, and non-Gaussian step-size distributions, suggested that interfacial transport in the presence of highly viscous oil was dominated by desorption-mediated hopping, where a polymer chain desorbs from the interface, undergoes an excursion into the bulk liquid (with potentially multiple interfacial collisions),[6] and finally readsorbs at a new location, resulting in a hopping event. While this mechanism is also expected to be present at interfaces with less viscous oil, in this regime the desorption-mediated mode is slow compared to the more conventional Stokes−Einstein mode.

We therefore concluded that by varying the PDMS viscosity, one could transition from a regime where interfacial polymer diffusion was dominated by viscous drag to one where it was dominated by intermittent desorption-mediated diffusion. In the latter regime, the effective diffusion coefficient is largely

DOI: 10.1021/jacs.5b07108
J. Am. Chem. Soc. 2015, 137, 12312−12320

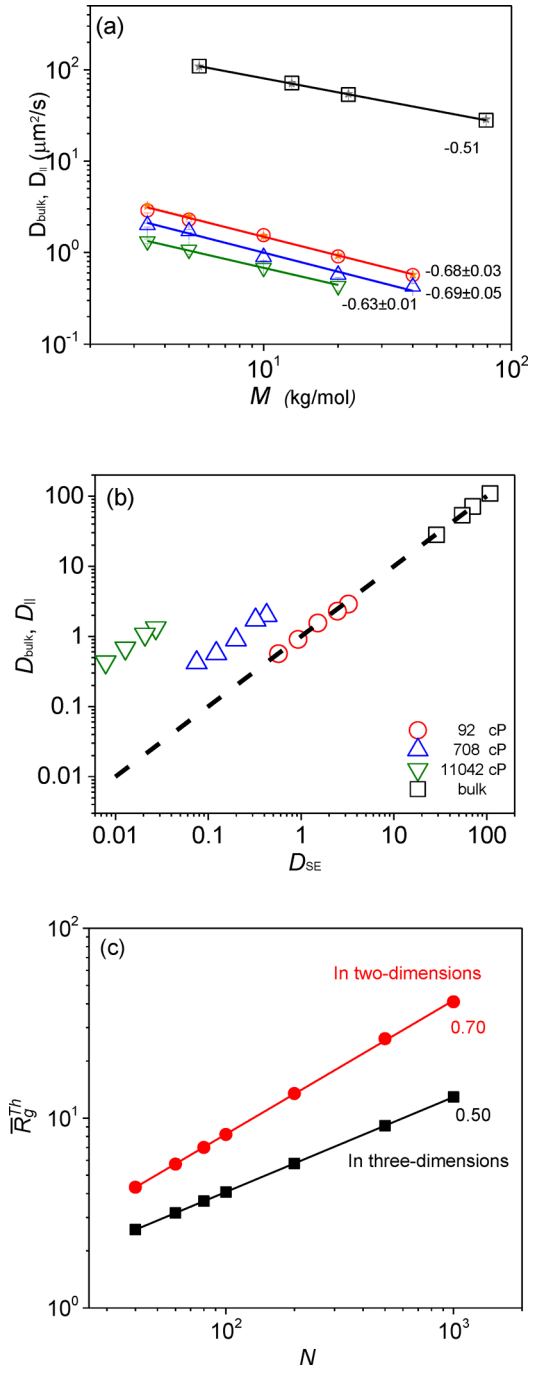

Figure 4. (a) Double logarithmic plot of the bulk, D_{bulk}, and interfacial, $D_{||}$, PEG diffusion coefficients versus molecular weight (M) in aqueous solution (squares) and at dilute coverage at the interface between water and PDMS with viscosities of 92 (circles), 708 (regular triangles), and 11042 cP (inverted triangles). The apparent interfacial diffusion coefficients were determined by analysis of MSD data as described in the text. The scaling exponents associated with each data set are annotated at right. The solid star symbols represent SCFT calculation results with $\overline{\nu}$ = 0 (gray) in three-dimensions and $\overline{\nu}$ = 1 (orange) in two-dimensions as described in the text. (b) Scatter plot of measured diffusion coefficients versus the theoretically expected Stokes–Einstein diffusion coefficients clearly showing two regimes of behavior. The dashed line indicates where the values of ordinate and abscissa are equal. (c) SCFT calculations of the relative dimensionless radius of gyration ($\overline{R}_g^{Th}$) for polymer chains as a function of degree of polymerization N with $\overline{\nu}$ = 0 in three-dimensions (solid black squares) and $\overline{\nu}$ = 1 in two-dimensions (solid red spheres).

determined by the characteristic frequency of desorption events. Interestingly, regardless of the dominant mechanism for interfacial diffusion, the measured interfacial diffusion coefficients exhibited similar scaling behavior, $D_{||} \sim M^{-2/3}$. Thus, we have proposed two distinct transport scenarios to interpret this dependence: one based on classic scaling theory for the radius of gyration (to explain the mobility in the Stokes–Einstein regime) and another in terms of the relation between the number of adsorbed monomers and the desorption energy (to explain the frequency of desorption-mediated flights). These two approaches were both consistent with a transition from random-walk chain conformations under θ-solvent conditions in bulk water to more expanded conformations associated with good solvent conditions upon adsorption at the oil–water interface. This is despite the fact that the oil phase is, overall, a poor solvent for the PEG polymer chains.

Scaling with Molecular Weight in the Stokes–Einstein Regime. Diffusion at the lowest viscosity PDMS–water interface (92 cP) was observed to be Fickian (linear MSD and Gaussian statistics), and the diffusion coefficients were well-described by the Stokes–Einstein relation, consistent with previous studies.[9] While it is likely that desorption–readsorption events also occurred at this interface, they apparently did not play a major role because of the fast dynamics of the in-plane diffusion. In the Stokes–Einstein regime, the diffusion coefficient obeys the relation $D \propto k_B T/\eta R_H$, where η is the effective viscosity of the medium and R_H is the hydrodynamic radius, which is approximately proportional to the radius of gyration, R_g. Therefore, combined with the conventional scaling relationship between radius of gyration and molecular weight, $R_g \propto M^{\nu}$, the diffusion coefficient is expected to exhibit the dependence $D \propto M^{-\nu}$ in the Stokes–Einstein regime.

In this context, the difference between the behavior of D_{bulk} and $D_{||}$ with molecular weight could be directly ascribed to a change in the polymer conformation in these different environments. In particular, the exponent ν = 0.5 in bulk water reflects Gaussian "random-walk" chain statistics nominally associated with a θ-solvent environment. The unusual scaling exponent of ν = 0.68 for PEG at the low viscosity interface clearly indicates a more expanded or swollen conformation compared to θ-solvent behavior. To put this into context, according to classical Flory theory,[2] a flexible chain in an idealized "good solvent" environment exhibits self-avoiding walk statistics; at a 2D interface this leads to $\nu = 3/(d + 2) = 0.75$, where d is the spatial dimensionality. While the measured exponent of 0.68 is obviously slightly smaller than this, it nevertheless indicates that the chains adopt conformations that are significantly expanded compared to a Gaussian chain and nearly as expanded as in an ideal good solvent. Since water is a θ-solvent for PEG (ν = 0.5) and the PDMS oil is a poor solvent for PEG (ν = 1/3), it is remarkable that the interface between these two solvents would represent an environment that apparently acts as a good solvent.

A modified SCFT using a specified test chain was proposed to quantitatively characterize the conformations in aqueous solution and the oil–water interface. SCFT has been a successful approach in determining polymer surface and interfacial properties.[2b,11b,19] Here, this modified SCFT was employed to study the bulk and interfacial conformations for a single linear polymer by fixing one end of a polymer chain at the origin in 2D and 3D systems. The self-consistent potential field $\mu(r) = \nu\rho(r)$ accounts for the effective interaction between

DOI: 10.1021/jacs.5b07108
J. Am. Chem. Soc. 2015, 137, 12312–12320

monomers in solvent, given the excluded volume parameter v. The full derivation is given in the Supporting Information. The generalized mean-square radius of gyration is given as $\langle R_g^{Th^2} \rangle = (1/2N)\int \omega(r) r^2 dV$, where N is the degree of polymerization and the integral represents volumetric integration over all space in two- or three-dimensions.

To determine the scaling law between the theoretical (dimensionless) radius of gyration, $\overline{R}_g^{Th} = R_g^{Th}/b$ and N, a series of polymers with different degrees of polymerization, ranging from $N = 40$ to 1000, were selected for SCFT calculations. The only adjustable parameter in our SCFT calculation was the dimensionless site−site excluded volume parameter $\overline{v} = v/b^3$ where b is the Gaussian statistical segment length used in the SCFT; $\overline{v} = 0$ indicates a zero net monomer interaction corresponding to θ-solvent conditions, while an increase of $\overline{v}$ indicates greater monomer repulsion. For the θ-solvent case, the SCFT calculations with $\overline{v} = 0$ generate random walk statistics, and as shown in Figure 4c, the theoretical scaling exponent was consistent with Gaussian chain behavior, $\overline{R}_g^{Th} \sim N^{0.5}$.

To make a direct connection between this theoretical approach and the experiments at the oil−water interface, we assumed the theoretical (dimensionless) radius of gyration $\overline{R}_g^{Th} = R_g^{Th}/b$ was proportional to the measured hydrodynamic radius, $\overline{R}_g^{Th} = (\lambda/b)R_H$, where λ is a dimensionless factor. This combined scaling factor accounts for both the ratio between R_H and $\overline{R}_g^{Th}$ for a chain as well as the choice of the statistical segment length. Therefore, the parameter λ/b required to rescale the theory to the experiments was determined by a least-square fit to the experimental data for aqueous solution. Hence, $\lambda/b = 6\pi\eta\overline{R}_g^{Th}D_{bulk}/k_BT \approx 2.2$ nm^{-1}, where η is viscosity, and D_{bulk} is the experimentally measured diffusion coefficient of PEG in dilute aqueous solutions. Given this determination of the scaling factor, the theoretical diffusion coefficient in solution was determined using the expression $D_{SE} = k_BT\lambda/6\pi\eta\overline{R}_g^{Th}b$, as shown in Figures 4a (star symbols) and S5 (star symbols with dashed lines).

The adaptation of the SCFT algorithm to two dimensions required the definition of a different characteristic length scale, of $b_{2d} = (2/3)^{1/2}\, b_{3d}$. As a result, the length scale λ/b_{2d} required to rescale the theory to the interfacial experiments was determined to be 2.7 nm^{-1}. To model the chain swelling at the interface, we applied the 2D algorithm with a positive excluded volume parameter, $\overline{v} = v/b^2 = 1$, to account for steric repulsion between monomers at the interface. The scaling of, $\overline{R}_g^{Th}$ vs N in a log−log plot yielded, $\overline{R}_g^{Th} \sim N^{0.70}$, (as shown in Figure 4c), indicating a swollen/expanded molecular conformation with decreased monomer density (Figure S4), signifying that the polymer chain was in a good solvent environment. Using $\overline{v} = 1$ and $\lambda/b_{2d} = 2.7$ nm^{-1}, Figure 4a shows excellent agreement between the experimentally measured $D_{||}$ and the theoretical diffusion coefficients calculated by the Stokes−Einstein relation for a disk at an interface,[17] $D_{SE,||} = 3k_BT\,\lambda/16b_{2d}\overline{R}_g^{Th}(\eta_{oil} + \eta_{water})$, where η_{water} and η_{oil} are the viscosities of the water and PDMS phases, respectively. Moreover, we found that the parameters $\overline{v}$ and λ/b_{2d} were coupled in their influence on the consistency between the SCFT and the experimental results. For example, using $\overline{v} = 2$ and a larger prefactor $\lambda/b_{2d} = 3.1$ nm^{-1}, we also obtained an adequate fit in agreement with the same experimental data. A larger λ/b_{2d} is expected since the SCFT algorithm assumed an exact 2D conformation at the interface with effective radii likely larger than a polymer with loop−train−tail conformation, as described below. It appears that $\overline{v}$ in the range of 1−2 can adequately represent the experimental data, consistently indicating a partially swollen conformation.

Reconciling the Scaling with Molecular Weight in the Intermittent Hopping Regime. SCFT has provided us a quantitative framework to understand the conformation of the polymer at the oil−water interface in this work and supported the view that the conformation is similar to that of a self-avoiding random walk. Polymer scaling theory based on Monte Carlo studies of self-avoiding random walks has also shown that polymer conformations should be expanded at ideal solid−liquid interfaces and have identified the polymer conformation as a sequence of surface-adsorbed trains and unadsorbed loops and tails.[10c,20] At a solid surface, the number of adsorbed monomers in a chain of length N scales as $N^{0.6\pm0.2}$, according to simulations.[20] Notably, we do not expect the conformation to have a significant dependence on oil viscosity, since the chemical attraction between the oil and the PEG should be independent of viscosity. Therefore, it is instructive to ask how the same molecular conformations can lead to similar scaling behavior in dramatically different regimes of interfacial transport.

In this study, we observed scaling of $D_{||} \sim N^{0.68}$, at low PDMS viscosity where the diffusion followed a Stokes−Einstein mechanism. In the usual description of interfacial Stokes−Einstein diffusion, the molecule at the interface is modeled as a disk with a characteristic hydrodynamic radius, which is expected to scale like the 2D projection of the molecular radius of gyration, $R_{g,||}$. For adsorbed flexible chains, $R_{g,||}$ is predicted to scale with molecular weight with a power law exponent that evolves from the value in solution ($\nu = 0.5$ in this case) to the value for a 2D self-avoiding walk ($\nu = 0.75$) as the strength of the monomer-surface interaction increases (or, equivalently, as temperature decreases). Thus, the exponent observed here, $\nu = 0.68$, represents an intermediate conformation, consistent with what has become known as a train−loop−tail conformation (Figure 5). This is not entirely surprising since water is a much better solvent for relatively polar PEG than PDMS[21] so that PEG penetration into the PDMS phase should be minimal.

Using high-viscosity PDMS, we observed surprisingly fast diffusion, suggesting that an additional mechanism for diffusion was present. In a previous study of protein diffusion at the PDMS−water interface,[9b] the interfacial diffusion coefficient was found to agree with the Stokes−Einstein relation at low oil

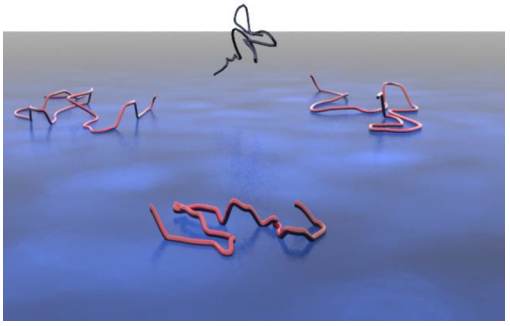

Figure 5. (a) Artistic presentation of adsorbed polymer chains (red) adopting a swollen (loop−train−tail) interfacial conformation compared to the one in bulk liquid (black).

DOI: 10.1021/jacs.5b07108
J. Am. Chem. Soc. 2015, 137, 12312−12320

viscosities but to become anomalously high at high oil viscosities, similar to our observations here. In that study, the magnitude of the diffusion coefficient at the highest viscosity was similar to that measured on a solid hydrophobic surface, on which desorption-mediated diffusion, i.e., hopping, had been observed.[9b,22] The authors suggested that hopping was then also occurring at the oil−water interface and becoming the dominant mechanism for interfacial diffusion at high oil viscosity. We conclude that the same transition from Stokes−Einstein to hopping interfacial diffusion is observed for PEG at the oil−water interface in the current experiments, and indeed the behavior for highly viscous oil was similar to that for PEG molecules on a hydrophobic solid surface.[4m]

In desorption-mediated diffusion, transport consists of two distinct processes: "waiting time" intervals where a molecule is bound to the interface and "flights" through the liquid phase (the aqueous phase in this case). Since diffusion through the bulk water is fast compared to the time scale of imaging, it is generally assumed that the time intervals associated with the flights represent a negligible fraction of the total. To verify this, for the highest viscosity oil, where transport is dominated by flights, we calculated the time required for a molecule to diffuse (in water) a distance corresponding to the longest observed flights (as an upper limit), using the diffusion coefficient extrapolated from the FCS measurements. This upper limit time interval varied between 4 and 7 ms (over the range of PEG molecular weights studied), which is much shorter than the acquisition time of 50 ms (obviously the vast majority of flights are dramatically shorter than these upper limits). Therefore, the primary contribution to the scaling of the diffusion coefficient in the hopping regime came from the dependence of the waiting times (i.e., the desorption rate) on the molecular weight. Consistent with this view, we have found that on a solid surface the diffusion coefficient scales in proportion to the desorption rate constant.[4m] Importantly, the desorption of the entire polymer from the surface can be thought of as a series of independent desorption events (the desorption of each train) if the trains are well-separated, such that hydrodynamic interactions between the trains are negligible.[23] The characteristic time associated with the desorption of a train is expected to be $\tau_{train} \sim \exp[l_{train}\varepsilon/k_BT]$, where l_{train} is the length of the train and ε is the binding energy of each polymer segment.[10a,b,d] The total desorption time for the polymer chain is therefore $n_{train}\tau_{train}$, where n_{train} is the number of trains per polymer chain. Eisenriegler et al. indicated that for a loop−train−tail conformation $n_{train} \sim N^{0.6}$.[10c] Thus, one expects the desorption time to scale as $N^{0.6}$, as we previously observed for PEG desorbing from a solid hydrophobic surface.[4m] In that case, we were able to measure the desorption rate on a solid surface by setting an empirical threshold, such that any apparent step greater than the threshold was assumed to have been the result of a desorption event. This was because the "infinitely high" viscosity of solid surface caused apparent molecular immobilization. Unfortunately, desorption rates cannot be directly measured at an oil−water interface using the same approach because adsorbed molecules can exhibit nonzero in-plane diffusion coefficients. So we must rely on the magnitude and scaling of the interfacial diffusion coefficient to infer interfacial conformation.

If the polymers are adsorbed in a train−loop−tail conformation as discussed above (Figure 5), then the desorption rate constant for PEG desorbing from the interface into the bulk water should scale in the range of $N^{-0.5} \sim N^{-1}$ and the diffusion coefficient should have the same scaling exponent. Indeed, with high viscosity oil, where the diffusion was clearly much faster than predicted for Stokes−Einstein diffusion, the diffusion coefficient scaled as $N^{-0.63}$, suggesting that the molecules adsorbed in a loop−train−tail conformation. Thus, a loop−train−tail conformation at the oil−water interface explains the scaling we have seen at both high and low viscosities and is in good agreement with previous studies of interfacial diffusion.[9,18]

One might expect the relevance of these results to extend to other interfaces, e.g., the air−water interface, which is often considered a special case of a hydrophobic interface. Given the low viscosity of both air and water, hopping would be expected to have a minimal contribution in this case, and the diffusion is likely controlled by viscous drag. Unfortunately, there is limited experimental information about the diffusion of isolated chains at the air−water interface. In early work, Lüdtke et al. studied the diffusion coefficient of poly(2-methyl-2-oxazoline) at the air−water interface in the dilute regime[24] and reported an exponent of −1, which is obviously quite different from the behavior observed here. The authors suggested that this behavior was consistent with Rouse dynamics. However, it should be noted that this exponent was extrapolated from only two molecular weights, and the polymers were strongly anchored to the interface via a covalently tethered lipid moiety, so a direct comparison with the current results is difficult. Additional studies of isolated chain dynamics and conformation at the air−water interface would certainly be of interest.

Microscopic Interpretation. Given that PEG is a Gaussian chain in aqueous solutions, and PDMS does not dissolve PEG, the PEG chain would not be expected to swell in the bulk of either substance. However, in the results reported here, we have found that PEG swells at the PDMS−water interface. A possible rationale for this involves molecular-level amphiphilicity of PEG which results in unique conformations at the oil−water interface. One hypothesis involves the favorable interaction of the ether groups with water due either to polar or hydrogen bonding interactions, while the methylene moieties are obviously hydrophobic and attracted to the PDMS phase. Moreover, surface reorientation of C−O bonds of PDMS can work synergistically with ether bonds of PEG through dipole−dipole interactions to further expand PEG chains. Therefore, at the PDMS−water interface, the methylene and ether moieties are each favored by one phase, respectively, potentially leading to unique conformations reflective of a good solvent environment. Comparatively, in bulk water, the hydrogen-bonding interactions are balanced by the repulsive interaction between hydrocarbon groups and water, giving rise to a small net interaction. In an alternative conceptual approach, inspired by interfacial particle adsorption,[25] an amphiphilic polymer is expected to occupy as much surface area as possible to decrease the surface free energy. The spirit of this concept has been observed recently in a molecular dynamic simulation for single amphiphilic molecules at an air−water interface.[26]

Since the silicone oils used in these experiments all comprise PDMS oligomers, a reasonable first approximation treats them as chemically similar to only the viscosity varying. However, there are likely some subtle effects associated with the molecular weight that could influence the structure and interactions of PEG with the oil interface. We cannot rule out the possibility that these subtle changes may influence the interfacial conformation of PEG. For example, since the driving

DOI: 10.1021/jacs.5b07108
J. Am. Chem. Soc. 2015, 137, 12312−12320

force of PEG adsorption is related to the hydrophobic interaction, the subtle change of hydrophobicity associated with PDMS molecular weight could potentially influence the configuration of adsorbed chains. Obviously, the data presented here do not directly address these issues, and we hope that this study will motivate subsequent theoretical and experimental efforts to resolve the polymer conformation in atomistic detail and the conformational evolution in response to the change of interfacial properties.

CONCLUSIONS

High-throughput molecular tracking was used to study the interfacial diffusion of PEG, with varying molecular weights, at the PDMS−water interface. At the interface with low-viscosity PDMS, PEG exhibited simple Brownian diffusion, where the diffusion coefficient was determined by viscous drag, exhibiting Stokes−Einstein behavior. However, at interfaces with high-viscosity oil, the absolute interfacial mobility was much faster than expected and consistent with intermittent hopping transport as observed at the solid−liquid interface. Interestingly, regardless of the dominant mechanism for interfacial diffusion, the measured scaling at the interface was approximately $D \sim M^{-2/3}$. Compared to diffusion in dilute aqueous solution, which exhibited θ-solvent behavior ($D_{bulk} \sim M^{-1/2}$) suggesting ideal chain conformations, both theory and experiments in these widely varying diffusive regimes were consistent with interfacial PEG chains having swollen conformations corresponding to "good solvent conditions". This conformational change upon adsorption from bulk solution to an interface should be considered in the design and manipulation of polymer materials at hydrophobic interfaces.[27]

ASSOCIATED CONTENT

Supporting Information

The Supporting Information is available free of charge on the ACS Publications website at DOI: 10.1021/jacs.5b07108.

Materials, sample preparation, experimental details, supplemental figures and supplemental note for SCFT calculation (PDF)

AUTHOR INFORMATION

Corresponding Author

*daniel.schwartz@colorado.edu

Notes

The authors declare no competing financial interest.

ACKNOWLEDGMENTS

The authors acknowledge Dr. Jingfa Yang for the help of the modification of hydroxyl terminus PEG and Chen Wang for the rheological measurements. The authors also thank the U.S. Department of Energy Basic Energy Sciences, Chemical Sciences, Geosciences, Biosciences Division (DE-SC0001854) for support of D.W. and the National Science Foundation (Award CHE-1306108) for the development of methods and instrumentation used in this research.

REFERENCES

(1) Rubinstein, M.; Colby, R. *Polymers Physics*; Oxford University Press: Oxford, U.K., 2003.

(2) (a) Flory, P. J. *Principles of polymer chemistry*; Cornell University Press: Ithaca, NY, 1953. (b) De Gennes, P.-G. *Scaling concepts in polymer physics*; Cornell university Press: Ithaca, NY, 1979.

(3) Fetters, L.; Hadjichristidis, N.; Lindner, J.; Mays, J. *J. Phys. Chem. Ref. Data* **1994**, *23*, 619−640.

(4) (a) Milchev, A.; Binder, K. *Macromolecules* **1996**, *29*, 343−354. (b) Maier, B.; Radler, J. O. *Phys. Rev. Lett.* **1999**, *82*, 1911−1914. (c) Maier, B.; Radler, J. O. *Macromolecules* **2000**, *33*, 7185−7194. (d) Sukhishvili, S. A.; Chen, Y.; Muller, J. D.; Gratton, E.; Schweizer, K. S.; Granick, S. *Nature* **2000**, *406*, 146−146. (e) Sukhishvili, S. A.; Chen, Y.; Müller, J. D.; Gratton, E.; Schweizer, K. S.; Granick, S. *Macromolecules* **2002**, *35*, 1776−1784. (f) Zhao, J.; Granick, S. *J. Am. Chem. Soc.* **2004**, *126*, 6242−6243. (g) Desai, T.; Keblinski, P.; Kumar, S.; Granick, S. *Phys. Rev. Lett.* **2007**, *98*, 218301. (h) Qian, H.-J.; Chen, L.-J.; Lu, Z.-Y.; Li, Z.-S. *Phys. Rev. Lett.* **2007**, *99*, 068301. (i) Mukherji, D.; Bartels, G.; Müser, M. *Phys. Rev. Lett.* **2008**, *100*, 068301. (j) Ramadurai, S.; Holt, A.; Krasnikov, V.; van den Bogaart, G.; Killian, J. A.; Poolman, B. *J. Am. Chem. Soc.* **2009**, *131*, 12650−12656. (k) Wong, J. S. S.; Hong, L.; Bae, S. C.; Granick, S. *Macromolecules* **2011**, *44*, 3073−3076. (l) Shen, L.; Adachi, T.; Vanden Bout, D.; Zhu, X. Y. *J. Am. Chem. Soc.* **2012**, *134*, 14172−14178. (m) Skaug, M. J.; Mabry, J. N.; Schwartz, D. K. *J. Am. Chem. Soc.* **2014**, *136*, 1327−1332. (n) Klein Wolterink, J.; Barkema, G.; Cohen Stuart, M. *Macromolecules* **2005**, *38*, 2009−2014. (o) Cooper, J. T.; Harris, J. M. *Anal. Chem.* **2014**, *86*, 7618−7626.

(5) Kisley, L.; Chen, J.; Mansur, A. P.; Shuang, B.; Kourentzi, K.; Poongavanam, M.-V.; Chen, W.-H.; Dhamane, S.; Willson, R. C.; Landes, C. F. *Proc. Natl. Acad. Sci. U. S. A.* **2014**, *111*, 2075−2080.

(6) Wang, D.; He, C.; Stoykovich, M. P.; Schwartz, D. K. *ACS Nano* **2015**, *9*, 1656−1664.

(7) (a) Yu, C.; Guan, J.; Chen, K.; Bae, S. C.; Granick, S. *ACS Nano* **2013**, *7*, 9735−9742. (b) Skaug, M. J.; Mabry, J.; Schwartz, D. K. *Phys. Rev. Lett.* **2013**, *110*, 256101.

(8) (a) Bychuk, O. V.; O'Shaughnessy, B. *J. Phys. II* **1994**, *4*, 1135−1156. (b) Bychuk, O.; O'Shaughnessy, B. *Phys. Rev. Lett.* **1995**, *74*, 1795−1798. (c) Chechkin, A. V.; Zaid, I. M.; Lomholt, M. A.; Sokolov, I. M.; Metzler, R. *Phys. Rev. E* **2009**, *79*, 040105. (d) Bénichou, O.; Loverdo, C.; Moreau, M.; Voituriez, R. *Rev. Mod. Phys.* **2011**, *83*, 81−129. (e) Chechkin, A. V.; Zaid, I. M.; Lomholt, M. A.; Sokolov, I. M.; Metzler, R. *Phys. Rev. E* **2012**, *86*, 041101. (f) Berezhkovskii, A. M.; Dagdug, L.; Bezrukov, S. M. *J. Chem. Phys.* **2015**, *143*, 084103.

(9) (a) Walder, R. B.; Honciuc, A.; Schwartz, D. K. *J. Phys. Chem. B* **2010**, *114*, 11484−11488. (b) Sriram, I.; Walder, R.; Schwartz, D. K. *Soft Matter* **2012**, *8*, 6000−6003.

(10) (a) Scheutjens, J.; Fleer, G. *J. Phys. Chem.* **1979**, *83*, 1619−1635. (b) Scheutjens, J.; Fleer, G. *J. Phys. Chem.* **1980**, *84*, 178−190. (c) Eisenriegler, E.; Kremer, K.; Binder, K. *J. Chem. Phys.* **1982**, *77*, 6296−6320. (d) Wang, Y.; Rajagopalan, R.; Mattice, W. *Phys. Rev. Lett.* **1995**, *74*, 2503−2506.

(11) (a) Doi, M.; Edwards, S. F. *The theory of polymer dynamics*; Oxford University Press: Oxford, U.K., 1988. (b) Helfand, E.; Tagami, Y. *J. Polym. Sci., Part B: Polym. Lett.* **1971**, *9*, 741−746.

(12) Walder, R.; Schwartz, D. K. *Soft Matter* **2011**, *7*, 7616−7622.

(13) Walder, R.; Kastantin, M.; Schwartz, D. K. *Analyst* **2012**, *137*, 2987−2996.

(14) (a) Israelachvili, J. N. *Intermolecular and surface forces*, revised 3rd ed.; Academic Press: London, U.K., 2011. (b) Horinek, D.; Serr, A.; Geisler, M.; Pirzer, T.; Slotta, U.; Lud, S.; Garrido, J.; Scheibel, T.; Hugel, T.; Netz, R. *Proc. Natl. Acad. Sci. U. S. A.* **2008**, *105*, 2842−2847.

(15) (a) Klafter, J.; Sokolov, I. M. *First steps in random walks: from tools to applications*; Oxford University Press: Oxford, U.K., 2011. (b) Metzler, R.; Jeon, J. H.; Cherstvy, A. G.; Barkai, E. *Phys. Chem. Chem. Phys.* **2014**, *16*, 24128−24164.

(16) Koynov, K.; Butt, H.-J. *Curr. Opin. Colloid Interface Sci.* **2012**, *17*, 377−387.

(17) Ranger, K. B. *Int. J. Multiphase Flow* **1978**, *4*, 263−277.

(18) Yang, J.; Zhao, J.; Han, C. C. *Macromolecules* **2008**, *41*, 7284−7286.

DOI: 10.1021/jacs.5b07108
J. Am. Chem. Soc. 2015, 137, 12312−12320

(19) (a) Fleer, G.; Cohen Stuart, M. A.; Scheutjens, J. M. H. M.; Cosgrove, T.; Vincent, B. *Polymers at interfaces*; Chapman and Hall: London, U.K., 1993. (b) Walton, D.; Mayes, A. *Phys. Rev. E: Stat. Phys., Plasmas, Fluids, Relat. Interdiscip. Top.* **1996**, *54*, 2811. (c) Wu, D. T.; Fredrickson, G. H.; Carton, J. P. *J. Chem. Phys.* **1996**, *104*, 6387−6397. (d) Fredrickson, G. H. *The equilibrium theory of inhomogeneous polymers*; Oxford University Press: Oxford, U.K., 2006. (e) Matsen, M. W. *Soft Matter* **2006**, *1*, 87−178. (f) van Eijk, M. C. P.; Leermakers, F. A. M. *J. Chem. Phys.* **1998**, *109*, 4592−4601. (g) Sing, C. E.; Zwanikken, J. W.; de la Cruz, M. O. *Phys. Rev. Lett.* **2013**, *111*, 168303.
(20) Lai, P. Y. *Phys. Rev. E: Stat. Phys., Plasmas, Fluids, Relat. Interdiscip. Top.* **1994**, *49*, 5420−5430.
(21) Hill, R. M. *Curr. Opin. Colloid Interface Sci.* **2002**, *7*, 255−261.
(22) Walder, R.; Nelson, N.; Schwartz, D. K. *Phys. Rev. Lett.* **2011**, *107*, 156102.
(23) (a) Knight, J. D.; Lerner, M. G.; Marcano-Velázquez, J. G.; Pastor, R. W.; Falke; Joseph, J. *Biophys. J.* **2010**, *99*, 2879−2887. (b) Pastor, R. W.; Karplus, M. *J. Phys. Chem.* **1988**, *92*, 2636−2641.
(24) Ludtke, K.; Jordan, R.; Furr, N.; Garg, S.; Forsythe, K.; Naumann, C. A. *Langmuir* **2008**, *24*, 5580−5584.
(25) Binks, B. P.; Lumsdon, S. O. *Langmuir* **2000**, *16*, 8622−8631.
(26) Ishikawa, D.; Mori, T.; Yonamine, Y.; Nakanishi, W.; Cheung, D. L.; Hill, J. P.; Ariga, K. *Angew. Chem., Int. Ed.* **2015**, *54*, 8988−8991.
(27) (a) Kumaki, J.; Kajitani, T.; Nagai, K.; Okoshi, K.; Yashima, E. *J. Am. Chem. Soc.* **2010**, *132*, 5604−5606. (b) Sheiko, S. S.; Zhou, J.; Arnold, J.; Neugebauer, D.; Matyjaszewski, K.; Tsitsilianis, C.; Tsukruk, V. V.; Carrillo, J.-M. Y.; Dobrynin, A. V.; Rubinstein, M. *Nat. Mater.* **2013**, *12*, 735−740.

DOI: 10.1021/jacs.5b07108
J. Am. Chem. Soc. 2015, 137, 12312−12320